SAND99-0401J

Microscale Flow Modelling in Geologic Materials

Ruaidhrí M. O'Connor and Joanne T. Fredrich

Sandia National Laboratories, Albuquerque, New Mexico

Camera-ready Copy for

Physics and Chemistry of the Earth

Manuscript-No. SE 39.2-015

Offset requests to:
J.T. Fredrich
Geomechanics Department, MS-0751
Sandia National Laboratories
Albuquerque, NM 87185-0751
USA

DISCLAIMER

Journal: Physics and Chemistry of the Earth
MS No.: SE 39.2-015
First author: Ruaidhrí M. O'Connor

Microscale Flow Modelling in Geologic Materials

Ruaidhrí M. O'Connor and Joanne T. Fredrich
Sandia National Laboratories, Albuquerque, New Mexico

Received 23 November 1998 – Accepted YY February 1999

Abstract. Three-dimensional imaging techniques, numerical methods for simulating flow and transport, and emergent computational architectures are combined to enable fundamental studies of fluid flow at the pore scale. High resolution reconstructions of porous media obtained using laser scanning confocal microscopy reduce sampling artifacts to sub-micron features, and simultaneously capture multiple grain length scales. However, the volumetric image data sets are extremely large, and there are significant computational challenges in utilising this information effectively. The principal problem lies in the complexity of the geometry and the retention of this structure in numerical analyses. Lattice Boltzmann (LB) methods provide a direct means to simulate transport processes in complex geometric domains due to the unique ability to treat accurately and efficiently the multitude of discrete boundary conditions. LB methods are numerically explicit as formulated, and this characteristic is exploited through a mapping of the numerical domain to distributed computing architectures. These techniques are applied to perform single phase flow simulations in 3D data sets obtained from cores of Berea sandstone using confocal microscopy. Simulations are performed using both a purpose-built distributed processor computer and a massively parallel processer (MPP) platform.

1 Introduction

The microscale flow characteristics of most geologic materials are not spatially uniform. In particular, the heterogeneous nature of the pore space may cause the flow to be carried nonuniformly, such that it is affected critically by the local geometry and topology (typically, there is a distribution of pore and throat sizes, with variable connectivity and cooordination), e.g., David (1993); Fredrich et al. (1993). Using 2D network models, David (1993) found that for heterogeneous pore systems, only a small number of preferential paths carry the majority of the fluid flow. Earlier, Agrawal et al. (1991) found indirectly a similar result by artificially obstructing the first percolating path in Berea sandstone, and then measuring the effect on the bulk permeability. For coupled multi-phase or multi-physics processes, the geometry of fluid flow likely becomes even more complex and significant to the macroscopic behavior.

The purpose of the work described here is to develop a coupled experimental-computational framework to simulate pore-scale transport processes in geologic and engineering materials. The intention is to use this system to gain an understanding of the fundamental nature of flow and transport in complex porous media to complement the laboratory-scale experiments on which we rely currently. The present focus is on single phase, incompressible flows, although we aim to extend this framework to simulate the multiphase flows and coupled processes that are even less amenable to experimental investigation.

To capture and understand how the microstructural geometry affects the creation of preferential paths and their topology, high resolution reconstructions of porous media are obtained using laser scanning confocal microscopy (LSCM), Fredrich et al. (1995); Fredrich (1999). This technique provides a means to characterise accurately pertinent microstructural characteristics, including first order properties such as porosity and specific surface area, as well as higher order statistical metrics that characterise spatially distributed geometric aspects. The accuracy of the representation also facilitates the examination of scaling properties and the accurate characterisation of transport processes, e.g. permeability, dispersion, and multiphase flow.

Modelling flow in porous media using high resolution 3D images is a formidable challenge. The geo-

Correspondence to: J.T. Fredrich, MS-0751, Sandia National Laboratories, Albuquerque, NM 87185-0751

metric complexity (quantity of detail) oftentimes precludes the use of numerical techniques such as finite element (FEM), finite difference (FD), molecular dynamics (MD), or network modelling (NM). FEM is constrained by the quantity of storage required to discretise consistently the pore space (in the mathematical sense) and retain geometric detail. Smoothing (averaging) to achieve representative continuum elements (and numerical tractability) may erase the very features that dictate the evolution of the processes of interest. This is particularly true for multi-physics systems. While similar numerically to LB methods both in the manner in which the domain is discretised and the explicit numerical formulation, FD methods do not provide the mathematical framework in which to develop the multi-physics that are sought ultimately. Discretisation using MD requires meshing the pore geometry in the same manner as FEM, and then discretizing the fluid phase from a molecular length scale up to multiple pore lengths. The storage requirement alone is on the order of a terabyte of RAM per cubic micron of pore space. Using NM, it is possible to discretise the domain in a manner that retains the topology, but idealizes the geometry. Thus, while NM is a powerful tool for the qualitative study of flow paths in complex networks, it is not well suited for quantitative analysis of real systems.

Lattice Boltzmann (LB) methods are ideally suited for modelling phenomena at time and length scales intermediate to the continuum (macro) and molecular dynamics (micro) scales, that is, at the mesoscopic scale. LB methods do not suffer as severely from the discretisation constraints of FEM, but still require some ingenuity to be applied to the scale of real problems such as those considered here. To appreciate the computational obstacles involved, consider a typical data set obtained using confocal microscopy that consists of $768\times512\times128$ voxels ($\approx$50 million sites). In the standard LB formulation a voxel maps to a single lattice site, and to model the physics of interest, each site requires $\approx$100 bytes of state information. So while the meshing can be automated as a 1-to-1 mapping, a total of $\approx$5 gigabytes of memory is required. Because of the numerically explicit formulation, an additional constraint is introduced in that state information from each site must be transmitted to every other site before a steady state flow can be reached. For a data set of the size mentioned, it is not unusual to require of order $10^4 - 10^5$ iterations. On a modest scientific workstation $\approx0.25\times10^6$ sites per second might be processed, thus a data set of the above size would require weeks to months of CPU time. Of course this assumes that the data set can be represented in memory in the first place; in reality these spatio-temporal requirements render this technique unfeasible for application on a single workstation.

We overcome these constraints through two distinct but complementary innovations in the treatment of large data sets. The first is the derivation of a compression algorithm (a stencil of the pore space) to represent the geometry and simultaneously reduce the compute time. The second is the design of a cost effective hardware platform to store and compute tractably systems of this size. Combined, the two techniques permit the simulation of transport processes in large data sets over multiple pore length scales.

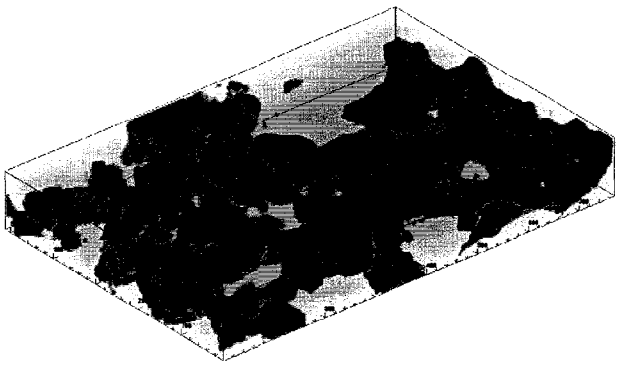

Fig. 1. Volume rendering of Berea sandstone used in LB simulation, with pore phase shown as opaque and solid phase as translucent. The image size is $768\times512\times101$ with cubic voxels of dimension 1 μm.

2 Three dimensional imaging

Volumetric image data were obtained using confocal microscopy, Fredrich (1999). To image porous media, the void space is filled with a fluorochrome-doped epoxy that is excited under laser illumination, and data consisting of fluorescence intensity are collected in xyz space. Following segmentation into solid and pore phases, the data are reconstructed to obtain the 3D geometry. In Fig. 1 we show a data set for Berea sandstone that is used in the simulations described here.

3 Lattice Boltzmann methods

LB methods are kinetic theory based techniques for simulating fluid flow that, for appropriate choices of energy distribution at the microscale, recover the Navier-Stokes and advection-diffusion equations at the macroscale. The microscale (in this model) consists of populations of fluid particles, n_i, associated with each site of a regular grid or lattice. The sites are connected with their neighbours through a set of prescribed numerical links that describe the paths for particle migration through the system. The number and spatial orientation of these links are defined by constraints on the symmetry and isotropy imposed by the underlying physics being modeled. Here we use the D3Q19 lattice, Qian et al. (1992).

The state of each site, i.e. velocity distribution, evolves according to the Boltzmann equation:

$$n_i(\mathbf{x}+\mathbf{e}_i, t+1) = \mathbf{\Omega}(n_i(\mathbf{x},t)) + n_i(\mathbf{x},t) \qquad (1)$$

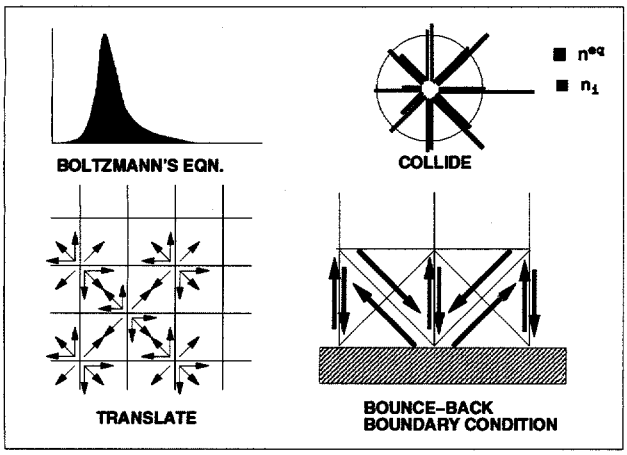

Fig. 2. Schematic illustration of LB method: (upper left) velocity distribution, (upper right) collision step, showing current versus equilibrium particle distribution along eight links in 2D (there are 18 links and a rest particle in 3D), (lower left) translation step, showing particle streaming along links to correct net imbalances, and (lower right) boundary condition at solid-fluid interface.

where $\mathbf{x}$ denotes a position in the lattice, $\mathbf{e}_i$ is the direction of link i, t is time, and $\mathbf{\Omega}$ is a Boltzmann collision operator. Eq. 1 can be decomposed into two parts, a collision term and a streaming (translation) term (Fig. 2). The collision term seeks to relax the local population of particles to equilibrium, and the streaming term migrates any net imbalance in the population to neighbouring sites along the prescribed links. Repeating these two steps over time allows the global system to evolve to an equilibrium or steady state condition.

In practice we use the linearised Bhatnagar, Gross and Krook (LBGK) form of the Boltzmann equation, Bhatnagar et al. (1954):

$$n_i(\mathbf{x}, t+1) = n_i(\mathbf{x}, t) + \frac{1}{\tau}[n_i^{eq}(\mathbf{x}, t) - n_i(\mathbf{x}, t)] + F_i(\mathbf{x}, t) \qquad (2)$$

As before n_i describes the particle populations at each site i, but the collision operator $\mathbf{\Omega}$ has been reduced to a linear expression in terms of the current distribution n_i and a prescribed equilibrium distribution n_i^{eq}. This linearisation is described as a single time-step relaxation where τ is the critical time step. In this expression we also show the term F_i that describes a forcing component used to drive the flow, e.g. gravity. Choosing a suitable equilibrium distribution, n^{eq}, allows one to recover Navier-Stokes flow at the macroscale, with stability over a range of Reynolds Number that bounds the flow regimes of interest in our work.

4 Distributed implementation

The porous media simulation framework is shown schematically in the form of a pipeline in Fig. 3. The pipeline starts with 3D image data acquired using LSCM, statistical analysis and characterisation, and geometric reconstruction of the porous medium as a binary (segmented) volume, Fredrich (1999). The reconstructed volume is the input to the flow simulation proper, that is, the sites describing the solid and void phases that together define the geometry of the connected pore space. These data are mapped onto the lattice in one of two ways.

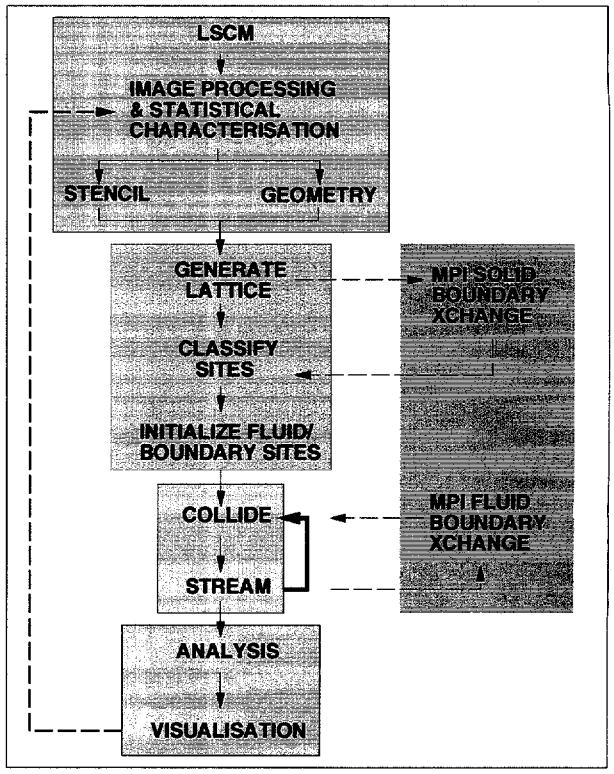

Fig. 3. Framework for studying flow in porous media.

In the traditional method, each binary voxel from the imaged domain is mapped onto a fully defined lattice site. Each voxel designates whether a site is treated as solid or void (containing fluid), but regardless of the phase, each site reserves sufficient memory to represent the fluid state. As the lattice is fully populated (defined), the binary data act as a mask designating whether the fluid physics at that site is included in the overall system and needs to be updated. So while this 1:1 mapping is straightforward and creates automatically a mesh of the geometry, it is very wasteful in terms of storage. Consider that the porosity of engineering materials is rarely $> 70\%$ and in the case of hydrocarbon-bearing sandstones, more typically $5 - 35\%$. That is, in many cases the majority of the domain consists of solid that does not take part in the flow simulation. Yet the traditional implementation reserves memory to represent the state of fluid at every site. Thus, for sandstone with porosity of say 20%, this approach wastes 80% of the allocated storage.

A second mapping approach, that we refer to as stenciling, was developed to address this problem. Although

more sophisticated, it nonetheless generates automatically a mesh consistent with the traditional approach. The essence of our method is to use the binary data set as a stencil for memory allocation and layout, rather than as a simple mask. That is, lattice memory is allocated only for sites that correspond to the void phase. Additionally, the location of the memory associated with each void voxel is encoded and stored in a corresponding location in a 3D image map on a site-by-site basis. With this approach, the algorithm traverses the image, and only when a site corresponding to void is encountered are the contents of the associated lattice memory accessed to determine the physics at that location. Thus, for Berea sandstone, this method enables the storage of models up to 5× larger with the same memory resource as the traditional approach. In the general case, the increase is equal to $1/\phi$ where ϕ is porosity. Because the stencil representation retains the surface description of the solid phase, it does not preclude application to coupled processes such as dispersion or multiphase flow. Multi-physics flows involving the solid phase (e.g., reactive flows such as precipitation/dissolution) clearly require the solid geometry to be mapped explicitly.

For the distributed implementation we developed algorithms to decompose the geometric domain so that subdomains are computed as separate processes. The decomposition was facilitated through use of a technique known as message passing, MPI (1995). Specifically, we use the MPICH library implementation of the *de facto* standard MPI, Gropp and Lusk (1997), to ensure portability to multiple hardware platforms. Message passing is a programming method that allows multiple processes to communicate with one another (whether they are running on the same processor, or on another processor connected over a network), in a way that makes the computation appear contiguous at the shared boundaries of the subdomains. A decomposition and communication pattern in a 2D domain is indicated schematically in Fig. 4. The arrows connecting the common internal boundaries show how neighbouring processes communicate. The arrows wrapping around the outer boundaries show the communication pattern for periodic flow conditions as described later. In Fig. 3 we show the message passing component of the pipeline as a parallel task to indicate that the simulation framework is independent of the underlying computer architecture. Message-passing operations are performed only if the system is computed on a distributed or parallel computer.

To initialise the system, copies of the shared boundary geometry and stencil information are sent to neighbouring processes (subdomains). The state of the fluid sites on the shared boundaries are also initialised by way of message passing so that consistent information is used to compute the flow physics.

The flow field is calculated iteratively, with the update loop consisting of two steps (Fig. 2). First the local physics are calculated for each fluid site using the collision term of Eq. 2. This establishes a new distribution of particles on each of the links. The second step is to translate (or stream) the contents of the links to nearest-neighbour lattice sites. This numerical communication extends to the boundaries of the subdomain, at which point an additional message passing step is performed to transmit information to neighboring subdomains.

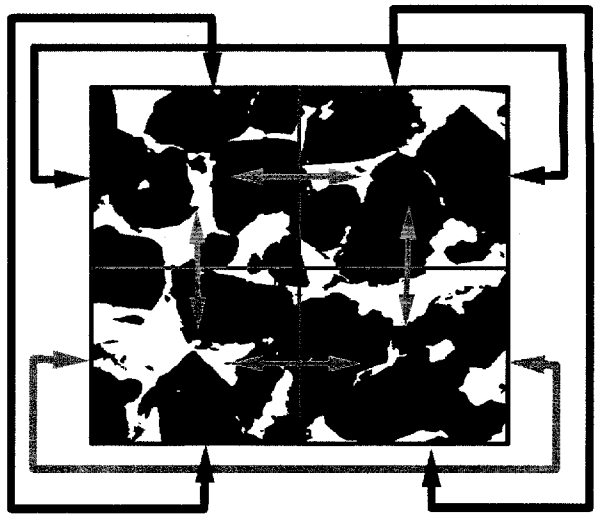

Fig. 4. Decomposition of a 2D domain into four subdomains, and showing communication between neighboring subdomains that is accomplished by message passing. In the 3D case, subdomains also communicate along two boundaries that would lie in the image plane. The implementation of periodic flow boundary conditions is shown with the arrows wrapping around the image area.

The system is computed in this way until a steady state is reached. This is recognised as a stabilisation of the local velocity and the decay of long range fluctuations over the domain. At this point the state of the system is analysed for the physical phenomena of interest, e.g. intrinsic permeability. An advantage of the coupled experimental-simulation technique is manifest in the rich data set that is derived. For example, it is possible to resolve the flow characteristics at a subpore scale (to voxel resolution). Finally, insight can be gained into the evolution and behaviour of the flow fields through use of 3D visualisation.

5 Flow boundary conditions

Two general forms of flow boundary conditions may be applied. The first defines sources and sinks at the boundaries to maintain a constant flow rate through the system. Realistic inflow conditions require a steady-state but spatially non-uniform velocity profile to match the effects of flow emanating from and being absorbed by neighbouring pore space. In general it is not possible to define this consistently without detailed *a priori* knowledge of the flow conditions at boundaries.

In the second form, flow is defined to be periodic at the boundaries (Fig. 4). Flow exiting the system is

wrapped around to the ingress. However, this approach is not locally consistent at the boundaries because of the inevitable geometric mismatch at the wrapped boundaries. To address this issue, the geometry is explicitly mirrored in the flow direction (doubling the x extent of the domain). Mirroring can also be introduced in the other two directions, either explicitly as in the flow direction, or, alternatively, by imposing symmetry boundary conditions. In the absence of a means to define consistent inlet-outlet or source-sink profiles, we have implemented the latter approach. (Note that symmetry and mirroring are not shown in either Figs. 4 or 5).

The remaining component of the LB implementation is the definition of a no-slip boundary condition to describe how fluid particles behave in the presence of solid obstacles (e.g., at pore walls). For simplicity the "bounce back" boundary condition is used. This rule was derived originally for Lattice Gas Automata, Cornubert et al. (1991), and is applied in a continuum form for LB. The premise is to reflect fluid particles impinging upon a solid wall (Fig. 2). While this is sufficient for modeling single-phase flow, a more complex treatment is necessary for modelling dispersion or multiphase flow, Noble et al. (1995); Chen et al. (1996). (For example, for dispersion, the carrier fluid is not characterised accurately in the boundary layer between the solid and void phase, leading to physical anomolies in solute transport.)

6 Distributed computing

As discussed above, the computation is intense and it is not possible to implement problems of the size considered here, $768\times512\times128$ ($\approx$50 million sites), on a standard scientific workstation. While supercomputing resources are available, regular and uninterrupted access to such resources is not typical.

To address the latter aspect, we used commercial off-the-shelf components to construct a 32-node distributed computer that can perform 9 GTOPS, with 8G of RAM, O'Connor and Fredrich (1997, 1999). Our system consists of two scalable units (SU) that each contain 16 computational nodes that are controlled by intermediate servers and I/O workstations. Each SU is connected using two layers of network; the control network is a 100bT ethernet switch, and the message passing (or compute) network, is formed using a 16-port Myricom© gigabit switch. We use the LINUX operating system, and all other utilities, libraries, and compilers are likewise public domain or freeware. The benefit of a cluster-based approach is realised clearly as an order of magnitude increase in resources for an order of magnitude decrease in cost (compared to vendor-specific parallel computing platforms). More specifically, this architecture can be used to replace standard commercial workstations (in terms of cost) while delivering an order of magnitude increase in resources (speed, memory, and storage).

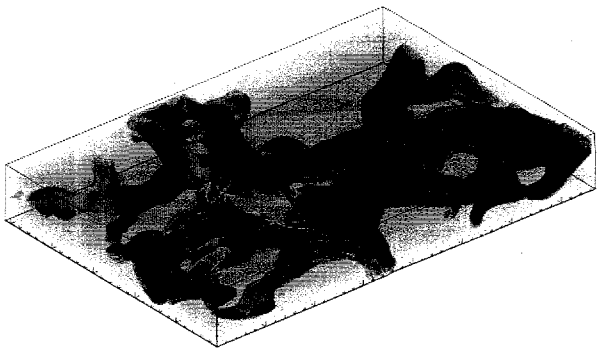

Fig. 5. Volume rendering of fluid velocity (magnitude) from LB simulation for Berea sandstone volume shown in Fig. 1. Colours indicate magnitude with red=high, green=intermediate, and blue=low.

With the cluster, we can run flow simulations for $\approx$100 million sites for representative porosities. However, extending the size of the data set further, or examining scaling properties requires use of supercomputing resources. We have used 512 nodes of the ASCI-Red (Teraflops) supercomputer to perform flow simulations in a data set sized $(768\times2)\times(512\times2)\times(128\times2) \approx 0.25$ billion sites, Fredrich and O'Connor (1998).

7 Application

We have applied our experimental-computational framework to model single phase fluid flow in 3D reconstructed volumes of Berea sandstone. Simulations have been performed for several data sets; here we show results for the volume shown in Fig. 1. Note that the flow is being driven in the x-direction that corresponds to the longest dimension in our model (i.e., 768 voxels as shown in Fig. 1). The complexity of flow patterns that arise in 3D "real" geometries prompted development of volume visualisation software. Fig. 5 shows a visualisation of the fluid velocity (magnitude) through the 3D reconstructed volume. The simulation reveals clearly accelerated flow in localized areas within pore bodies and through some pore throats, as well as the presence of low-velocity or "dead" regions within pore bodies where the flow is more than $10\times$ slower than that observed in high velocity zones.

The intrinsic permeability k can be calculated based on the standard Darcy formulation as indicated in Eqs. 3 and 4, where $\mathbf{U}_{Darcy}$ is the average fluid velocity over a cross-sectional area A_{yz} orthogonal to the pressure difference ΔP driving the flow, μ is the prescribed fluid viscosity, and $\mathbf{Q}$ is the volumetric flow rate through the medium. To drive the flow under gravity conditions one can define an equivalence between an applied body force F_x and the pressure difference experienced using Eq. 5. Substituting in Eq. 3 yields Eq. 6 that is used directly to derive k:

$$\mathbf{U}_{Darcy} = -(k/\mu)(\Delta P/\Delta x) \quad (3)$$

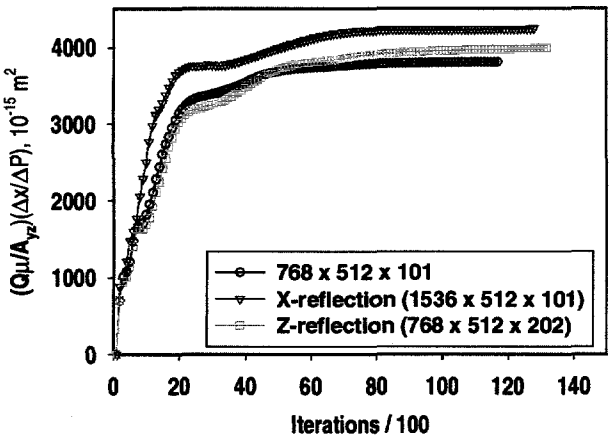

Fig. 6. Plot showing the evolution to a steady state permeability during the simulation. The simulation is for the reconstructed volume shown in Fig. 1, with different scaling as indicated.

$$\mathbf{Q} = \mathbf{U}_{Darcy} A_{yz} \quad (4)$$

$$\Delta P = -F_x \Delta x \quad (5)$$

$$k = \mu\, \mathbf{U}_{Darcy}/F_x = \mu\, \mathbf{Q}/F_x A_{yz} \quad (6)$$

The results from three simulations are shown in Fig. 6. The lowermost curve corresponds to the simulation on the basic reconstructed volume shown in Fig. 1. The uppermost curve corresponds to a simulation where the volumetric domain is reflected about the y-z plane in the direction of the flow (i.e., doubling the x-axis to 768×2). The middle curve is for a simulation where the volumetric domain has been reflected about the x-y plane, that is, doubling the minimum dimension of the model in the z-direction.

The range of k exhibited is approximately a factor of 3-5× the experimentally determined permeability of Berea sandstone. Because the data sets used correspond to a volume of 0.8 mm × 0.5 mm × 0.1 mm, one may expect the numerically derived permeability to be higher as there may be artificially connected flow paths that are either unconnected or else may not contribute to bulk flow in a larger sample, i.e. the image volume size may not capture all of the representative length scales.

These issues are currently being addressed by gathering multiple sample volumes from a single sample, by statistical analyses of the image data, and by numerical simulations on the imaged volumes. In addition, we are performing simulations on imaged volumes obtained from multiple samples of Fontainebleau sandstone with porosities that vary from 5% to 25% to compare more directly the computed versus simulated permeabilities.

8 Summary

We have created a coupled experimental-computational framework to integrate 3D imaging and numerical flow simulation techniques using approaches conducive for distributed computing. Our preliminary simulations examine single-phase flow in Berea sandstone, and our results, including numerical estimates of permeability, are encouraging. We achieve the tractable computation of large 3D data sets through development of a new storage algorithm to represent complex geometries, and by development of a distributed hardware platform. In combination, these advances increase dramatically the time and length scales over which transport processes can be simulated using commodity computer components.

Acknowledgements. We have benefitted from discussions with D. Noble, and thank an anonymous reviewer, J. Torczynski, and Y. Bernabe for comments on the original manuscript. Funding from the Engineering Sciences Research Foundation at Sandia (Laboratory Directed Research and Development Program), and the US DOE Office of Basic Energy Sciences (Geosciences Program) is gratefully acknowledged. This work was performed at Sandia National Laboratories funded by the US DOE under Contract DE-AC04-94AL85000. Sandia is a multiprogam laboratory operated by Sandia Corporation, a Lockheed Martin Company, for the United States Department of Energy.

References

Agrawal, D. L., Cook, N. G., and Myer, L. R., The effect of percolating structures on the petrophysical properties of Berea sandstone, *Proc. 32nd U.S. Rock Mech. Symp.*, pp. 345–354, 1991.

Bhatnagar, P., Gross, E., and Krook, M., A model for collision processes in gases. i. Small amplitude processes in charged and neutral one-component systems, *Phys. Rev.*, *94*, 511, 1954.

Chen, S. Y., Martinez, D., and Mei, R., On boundary conditions in lattice boltzmann methods, *Phys. Fluids, 8, 2527-2536*, 1996.

Cornubert, R., d'Humieres, D., and Levermore, D., A Knudsen layer theory for lattice gases, *Physica D*, *47*, 241–259, 1991.

David, C., Geometry of flow paths for fluid transport in rocks, *J. Geophys. Res.*, *98*, 12267–12278, 1993.

Fredrich, J. T., 3d imaging of porous media using laser scanning confocal microscopy with application to microscale transport processes, *Phys. Chem. Earth, XX*, YY–YY, this volume, 1999.

Fredrich, J. T. and O'Connor, R. M., Microscale flow modeling in reconstructed porous media, *Eos, Trans. Amer. Geophys. Un., v. 79, p. F895*, 1998.

Fredrich, J. T., Greaves, K. H., and Martin, J. W., Pore geometry and transport properties of Fontainebleau sandstone, *Int. J. Rock Mech. & Min. Sci.*, *30*, 691–697, 1993.

Fredrich, J. T., Menendez, B., and Wong, T. F., Imaging the pore structure of geomaterials, *Science*, *268*, 276–279, 1995.

Gropp, W. and Lusk, E., *MPICH 1.1.1: A Portable Implementation of the* **Message-Passing Interface** *Standard*, `www.mcs.anl.gov/mpi/mpich`, 1997.

MPI, *MPI: A Message-Passing Interface Standard, Version 1.1*, MPI Forum Technical Report, `www.mpi-forum.org`, 1995.

Noble, D. R., Chen, S., Georgiadis, J. G., and Buckius, R. O., A consistent hydrodynamic boundary condition for the lattice Boltzmann method, *Phys. Fluids*, *7*, 203–209, 1995.

O'Connor, R. M. and Fredrich, J. T., Araneæ- A scalable system for distributed computing, *Presented at the Scalable Cluster Computing Workshop, Monterey, CA, November 21-22*, 1997.

O'Connor, R. M. and Fredrich, J. T., Araneæ- A scalable system for distributed computing, *manuscript in preparation*, 1999.

Qian, Y., d'Humieres, D., and Lallemand, P., Lattice BGK models for the Navier-Stokes equation, *Europhys. Lett.*, *17*, 479, 1992.